**Design Fluxgate Magnetometer (Fluxgate Sensor)**

By

REATH BANAK REATH

Final Report

Submitted to the Electrical & Electronics Engineering Programme
in Partial Fulfillment of the Requirements
for the Degree
Bachelor of Engineering (Hons)
(Electrical and Electronics Engineering)

June 2009

Universiti Teknologi PETRONAS
Bandar Seri Iskandar
31750 Tronoh
Perak Darul Ridzuan

# CERTIFICATION OF APPROVAL

**Design Fluxgate Magnetometer (Fluxgate Sensor)**

by

REATH BANAK REATH

A project Final report submitted to the
Electrical and Electronics Engineering Programme
in partial fulfillment of the requirement for the
BACHELOR OF ENGINEERING (Hons)
(ELECTRICAL AND ELECTRONICS ENGINEERING)

Approved by,

Dr John.O.Dennis
Project Supervisor

UNIVERSITI TEKNOLOGI PETRONAS

TRONOH, PERAK

June 2009

## CERTIFICATION OF ORIGINALITY

This is to certify that I am responsible for the work submitted in this project, that the original work is my own except as specified in the references, and that the original work contained herein have not been undertaken or done by unspecified sources or persons.

Reath Banak Reath

## ABSTRACT

Fluxgate magnetometers have been used by robotic space probes to analyze, map and monitor the magnetic fields of the earth and other planets. They are also used in geological prospecting, aerospace navigation, underwater navigation, land navigation and submarine detection.

The objective of this project is to build fluxgate sensor for measuring a magnetic field, The fluxgate sensor has two ferromagnetic core, a primary, electrically conducting coil arranged around the core for periodical magnetization of the core into magnetic saturation by an alternating electric current through the primary coil, and a secondary, electrically conducting coil arranged around two ferromagnetic core.

The Methodology of the project has been carry out with precise decision in order to find a way to reduce the size, power consumption and cost, hence the author use low saturation flux density materials.

The design and testing of a fluxgate sensor, which is totally embedded in printed circuit board, has been presented. The sensor is suitable for sensing currents in the printed circuit board traces. The sensitivity has been measured at 150 mV/A for 50 kHz excitation. The power dissipation has been measured at approximately 1.44 W for a sinusoidal excitation. The power dissipation can almost certainly be reduced by using pulse excitation, or perhaps by using a saturable inductor in the excitation circuit. It is also possible to improve the sensitivity and reduce the power consumption by use of an improved magnetic material. In particular a material with lower saturation flux density and higher permeability should be possible.

Future work will focus on further characterization of the sensor in terms of bandwidth, noise level, and minimum current detection level.

**TABLE OF CONTENT**

## LIST OF FIGURES

**LIST OF TABLES**

# CHAPTER 1

# INTRODUCTION

## 1.1 Background Study

The fluxgate magnetometer is a magnetic field sensor for vector magnetic field [1]. Its normal range is suitable for measuring earth's field and it is capable of resolving well below one 10,000th of that. It has traditionally been used for navigation and compass work as well as metal detection and prospecting.

Fluxgate magnetometer designs fall into broadly two styles, those employing rod cores and those using ring cores. The rod cores were the first to be developed from about 1930 onwards, and the more convenient twin core design within this category is also split into two styles; the Forster [1] and Vaquier [2] based. The latter is the earliest design but continues to find favour in modern designs using the latest materials and electronics, as does the Forster variant. The ring core models although appearing in the 1930s [3] were not really developed until 1962 [4] on, when they were rapidly accepted as a serious contender to the rod core.

Fluxgate magnetometers have been used by robotic space probes to analyze, map and monitor the magnetic fields of the earth and other planets. They are also used in geological prospecting, aerospace navigation, underwater navigation, land navigation and submarine detection.

The heart of the fluxgate magnetometer is a ferromagnetic core surrounded by two coils of wire in a configuration resembling a transformer. Alternating current (AC) is passed through one coil, called the primary, producing an alternating magnetic field that induces AC in the other coil, called the secondary. The intensity and phase of the AC in the secondary are constantly measured.

When a change occurs in the external magnetic field, the output of the secondary coil changes. The extent and phase of this change can be analyzed to determine the intensity and orientation of the flux lines.

The technology is sometimes used in a comprehensive robot guidance system that operates on the basis of external magnetic fields. In such a system, navigation is guided by continuous analysis of the intensity and direction of the flux lines within the robot's work environment. Here's how it works: An artificial external reference field is generated by placing strong direct current (DC ) electromagnets at various points in the robot's work environment. The robot controller stores data concerning the resulting flux field. For each point in the work environment, the magnetic field has a specific intensity and the flux lines run in a specific direction. Based on this information, the robot can locate its position and orientation at all times and navigates along programmed paths.

Fluxgate magnetometers are usually employed in conjunction with other location and navigation methods such as the Global Positioning System (GPS ).

## 1.2 Problem Statement

Fluxgate magnetometers provide suitable sensitivity and resolution for the assigned tasks of littoral sensing. However, these devices are relatively expensive and not easily manufactured at quantity, two drawbacks when considering the number of devices required for desired deployment and sensor grid coverage. Therefore; it's very important to develop fluxgate magnetometer which is cheap and consumes low power.

## 1.3 Problem Identification

The problem identification can be represented in the following points based on the research coverage

- The very expensive cost of fluxgate sensor( Rod core fluxgate sensor)
- The high power consumption of fluxgate sensor( Rod core fluxgate sensor)

### a) Significance Of The Project

- Propose a solution that would minimize the cost and power consumption of the rod core fluxgate sensor
- Run experiments to investigate the fluxgate sensor at second harmonic voltage at different frequency
- The thesis would hopefully be distribute to company men and military personal for geomagnetic detection, military navigation and mine detection

### b) Objectives and Scope of Study

The overall objectives of the project are to design the fluxgate magnetometer sensor to detect the magnetic fields; therefore the main objectives are summaries below.

1. To study the fluxgate magnetometer and it's applications
2. Design and develop the excitation and detection circuit
3. Lab experiment testing of the fluxgate magnetometer

### C) The Relevancy of the Project

This project is relevant to the magnetic sensing of magnetic field, Military Navigation, metal detection and many others

### d) Feasibility of the Project within the Scope and Time

The feasibility is a achievable because, this project is not covering multi-scope research on the entire types of fluxgate sensors manufacture industry but it focus only the Rod core sensor (fluxgate sensor).

The project could be concluding within two semesters or less as long as the experiments are carried out to give the proposed evidence.

# CHAPTER 2

# LITERATURE REVIEW

## 2.1 Fluxgate Magnetometer

Fluxgate magnetometers have always been of interest to the technical and scientific communities as practical and convenient sensors for weak magnetic field measurements at room temperature, finding applicability in fields such as nondestructive testing, geophysical exploration and mapping, as well as assorted military applications. Recently, however, the possibilities offered by new technologies, materials, and readout schemes in realizing devices with improved performance, as well as miniaturization, and enhanced noise-tolerance, have lead to a renewed interest in fluxgate magnetometer technology for a variety of applications involving room temperature magnetic field measurements in the range of 0.01 mT or less.

In this sense, fluxgates fill the gap between squids that offer far greater sensitivity, but with significantly greater cost, as well as difficult operating conditions and the relatively inexpensive

Alternative technologies, based on the anisotropic magneto-resistance, giant magneto-resistance, and magneto-impedance effects, have been also recently studied in the context of precise magnetometers.

Fluxgate systems prevail over these competitive technologies not only because of their higher sensitivity but also because of lower noise level, robustness, and remarkable thermal and long-term stability.

## 2.2 Theory of Operation

The essential idea in this fluxgate magnetometer is to saturate the iron nickel wire with the excitation coil, when you place the wire in a small external magnetic field one part of the rod core device will saturate faster than the part opposing the magnetic field. The net magnetic induction will have fundamental frequency twice that of the external magnetic field along with higher even harmonics. This net voltage detected by the sense coil (some pulses) will be asymmetric and by Fourier analysis will consist of only even harmonics. A suitable filter can select out the second harmonic which will be proportional to the external (or bias) field. When we apply a periodic triangular voltage across the excitation coil this will cause a large magnetic field to be generated in the iron wire, so large that field will saturate in the iron wire, by Faradays law a voltage will be generated in the sense coil given by:

$$V_{SENSE} = -L\frac{dI}{dt} \propto \left(\frac{dB_{Excitation}}{dt} + \frac{dB_{Earth}}{dt}\right) \quad \text{..... (1).}$$

Where L is the mutual inductance of the pair of coils. A graph of the B field (in the upper wire in the rod core shaped device) and the voltage induced in the sense coil (from the upper wire in the rod core shaped device) is shown in figure 1. As you can plainly see the bottom curve (Voltage versus time) is proportional to the time derivative of the top curve (Magnetic Induction versus time).In a zero magnetic field, the magnetic induction and voltage induced in the sense coil by the bottom part of the rod core shaped device will be the mirror image (with respect to the time axis) of the graphs in figure 1 (if you wound the coil around the iron wire evenly and symmetrically).

Hence in a zero external magnetic field the sense coil should pick up no induced voltage since $V$Upper + $V$Lower _ 0. [5]

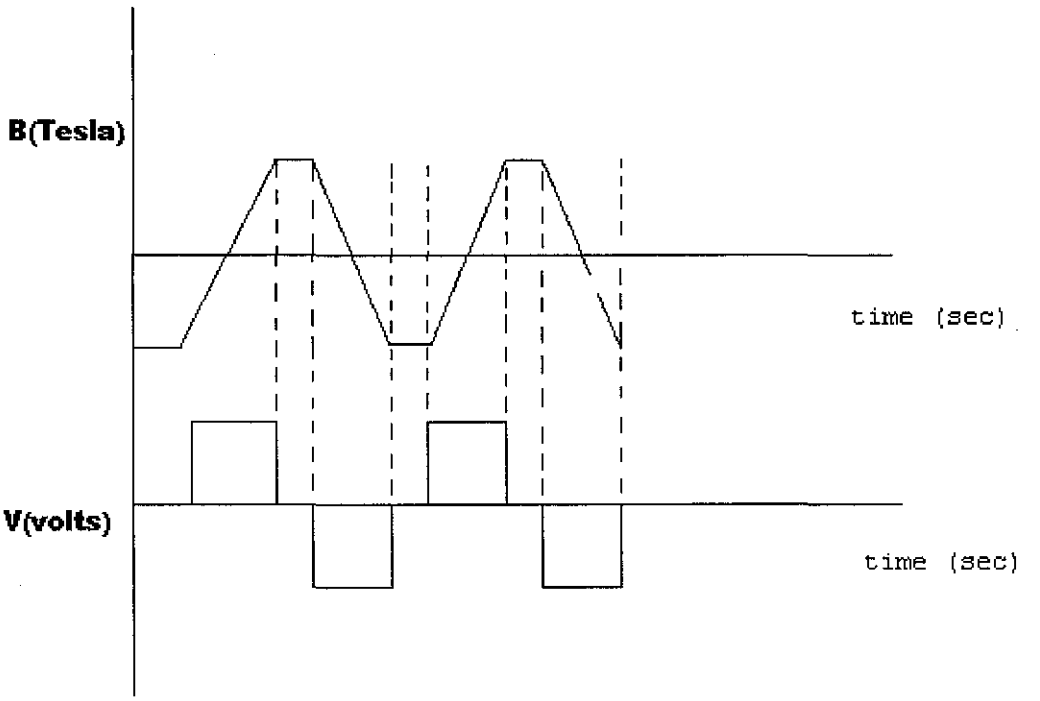


Figure 1: Saturate asymmetrically

When you place the detector in an external magnetic field (e.g. the Earth's magnetic field), the situation is now different. In this case the magnetic induction (B) in the coil will saturate asymmetrically in time, it will produce the waveform in figure 2.

Notice that the magnetic induction B saturates more quickly when the magnetic induction is in the same direction as the external magnetic field (the magnetic field you are trying to measure) compared to when the magnetic induction opposes the external field.

As you clearly see in figure 2, the flat parts of the magnetic induction (B) versus time curve is longer in the upper half of the graph and shorter in the bottom half of the graph.

The net voltage detected by the sense coil from the sum of the upper and bottom cores of your fluxgate magnetometer when it is placed in an external magnetic field will be a series of asymmetric pulses. As mentioned earlier these pulses will have a strong second harmonic component which can be filtered out and measured with the waveform analyzer and oscilloscope. [6]

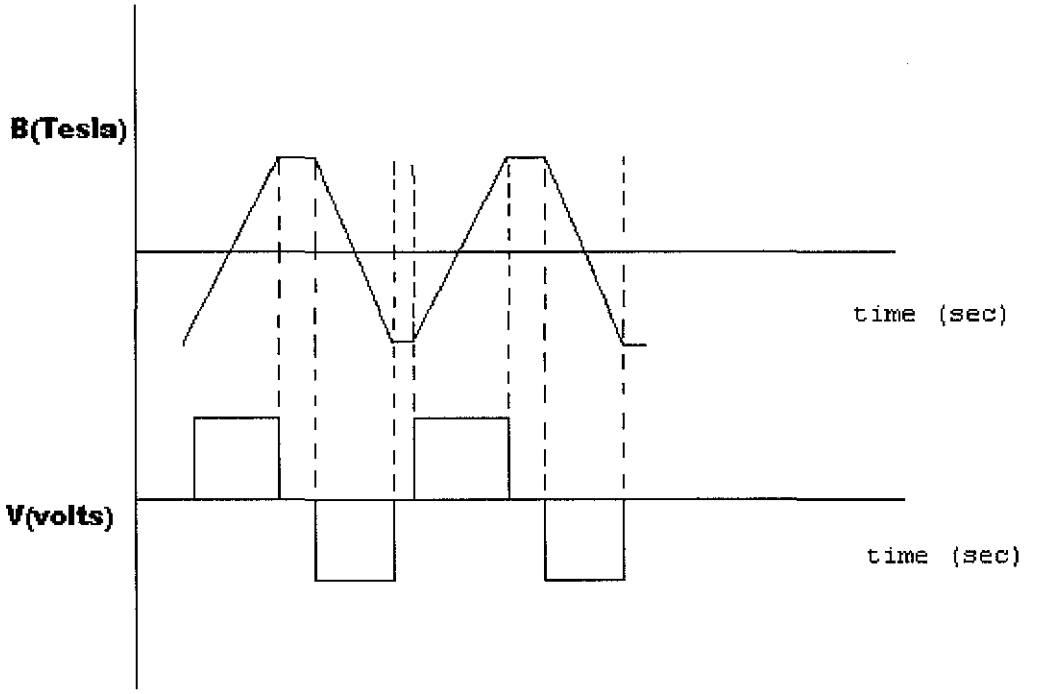


Figure 2: Saturate symmetrically

The Pasco waveform analyzer allows you select several types of filters and select various frequencies, you could in principle set the function generator to 10,000 Hz (or higher) and filter out the 20,000 Hz second harmonic. By Faradays law (equation 1) the induced voltage will be greater (since it depends on a time derivative) and hence more easily detected.

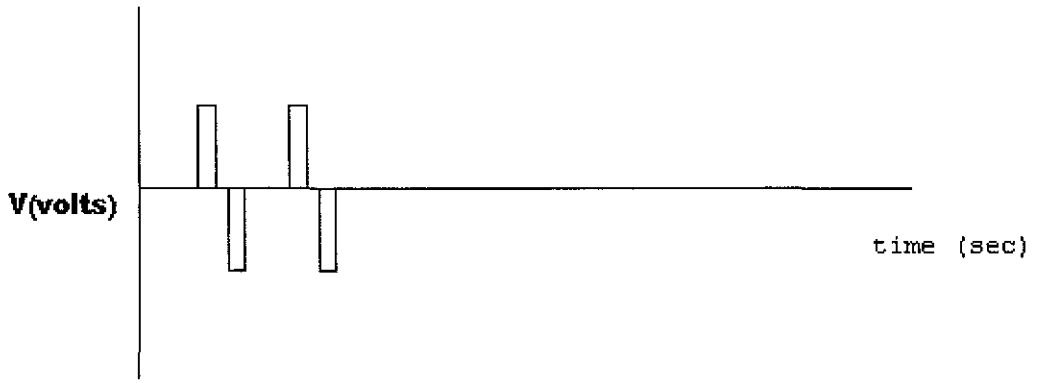


Figure 3: Second harmonic voltages

## 2.3 Magnetic Properties of the Ferromagnetic Wire

Fluxgate magnetometer uses iron wire of low magnetic coercively as one its key elements of operation. In this section we explain a few properties of magnetic materials necessary to understand its operation.

There are several types of magnetism (paramagnetic, diamagnetic and ferromagnetic).

The fluxgate magnetometer uses the ferromagnetic properties of the iron wire to work. Any ferromagnetic metal will exhibit nonlinear behaviour known as hysteresis. When you apply a magnetic field to a ferromagnetic material (such as iron) you will find that the magnetic induction in the material will at first increase linearly and then saturate at some external field, when you then reverse the field and try to demagnetize the iron, the magnetic induction in the iron will decrease but not retrace the original curve, you will get something like the hysteresis curve in figure 3. Hysteresis occurs because the iron

wire consists of many small magnetic domains, each domain with a magnetic moment pointing in a random direction.

By applying an external magnetic field and magnetizing the iron wire you will cause the magnetic domains to align along the applied external magnetic field.

The irreversibility of the magnetic domain alignment is the cause of the hysteresis and by the laws of thermodynamics heat will be created and energy lost.

Hysteresis is a problem for certain applications (e.g. transformer design) but in the fluxgate magnetometer application we are cleverly using it to our advantage. [7]

## 2.4 Rod Core design

The two common types of twin rod core design are shown below with the Forster based one on the left and the Vacquier on the right. These designs closely follow the design principles discussed above with differences only in the sense coil configuration.

The separate sense coils on the Forster design are phased such that they cancel the excitation while combining the signal voltages. It is possible to build a fluxgate based on the Forster using a common set of coils for excitation and sensing. Core material for the rod was traditionally high mu mu-metal wire. The rod is typically 20mm in length but can vary from 15 – 75mm.

These designs are good for directional sensitivity with the anisotropy of the core defining the sense direction, and are universally favoured by the geomagnetic community for their long term stability. This can be better than 3nT per year. [8]

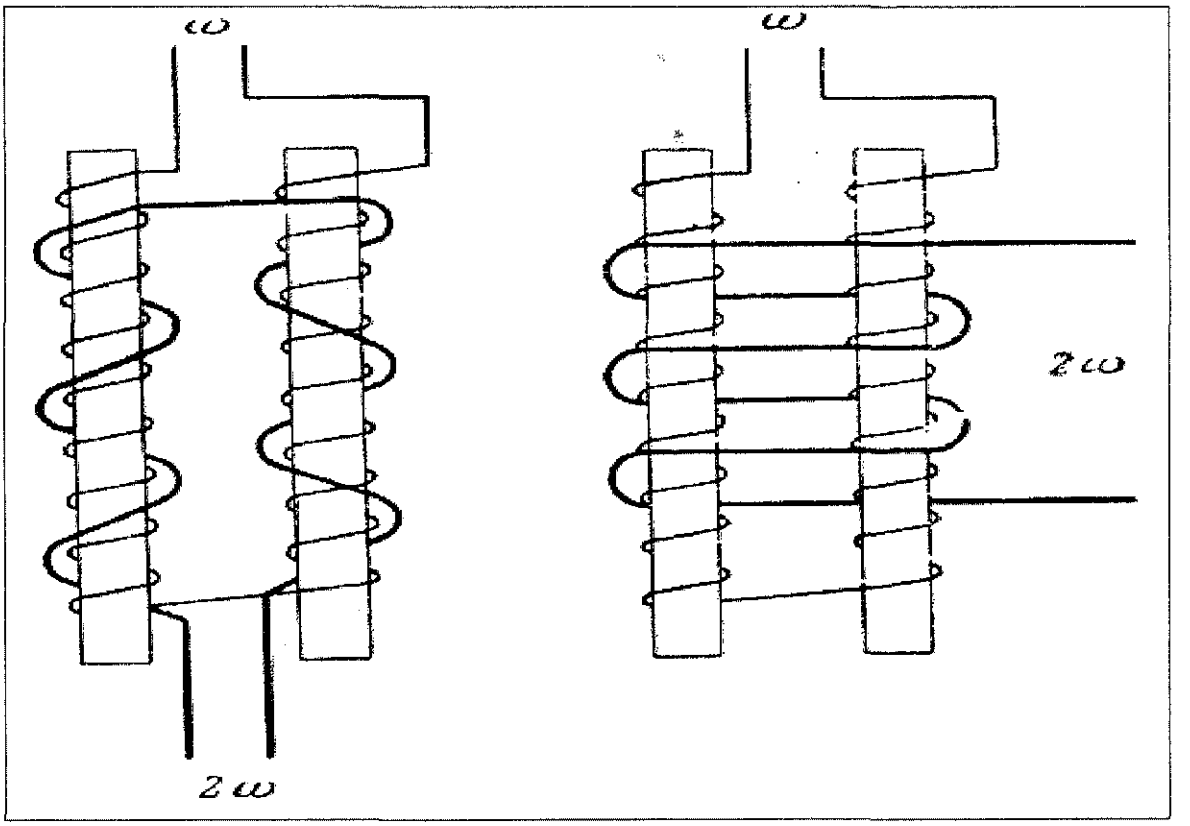


Figure 4: Different Rod core (fluxgate magnetometer) design

## 2.5 Fluxgate performance

The table below attempts to draw comparison between the various types of state of the art 2nd harmonic "twin core" fluxgates discussed in this document.

Where possible like is compared with like. For example similar size cores are compared for noise since it reduces as the size increases, and the core material is amorphous metal with the exception of the Ferrite ring. It is however still difficult to compare different sensor types because of variations in electronics employed. Stability of rod cores is regarded by the geomagnetic community, who have much experience in the use of fluxgates, as superior to that of ring cores.

Table 1: Comparison of performance of different fluxgate Sensor

| | Rod Core | Ring Core | Racetrack | Ferrite ring (commercial) |
|---|---|---|---|---|
| Noise/resolution | 46pT rms | 15pT rms | ~15pT rms | ~10, 000pT |
| Stability | *** | ** | | |
| Linearity | 10ppm | 10ppm | 10ppm | |
| Ease of manufacture | *** | ** | * | *** |
| Power needs | High | Low | Moderate | Moderate |
| Feed through | *** | ** | * | ** |
| Cross field | *** | * | *** | * |
| Perming | * | *** | ** | |

In theory the racetrack sensor should be the ultimate device with all the best points of the other two designs however it has little published data to corroborate the theory. On balance the ring core device is probably the higher performing of the three amorphous metal cored fluxgates, with excellent noise, resolution and low power requirements. Stability is arguably the equal of any design with crossfield effects remaining a possible. [9]

# CHAPTER 3

# METHODOLOGY

## 3.1 Procedures identification for the project studies

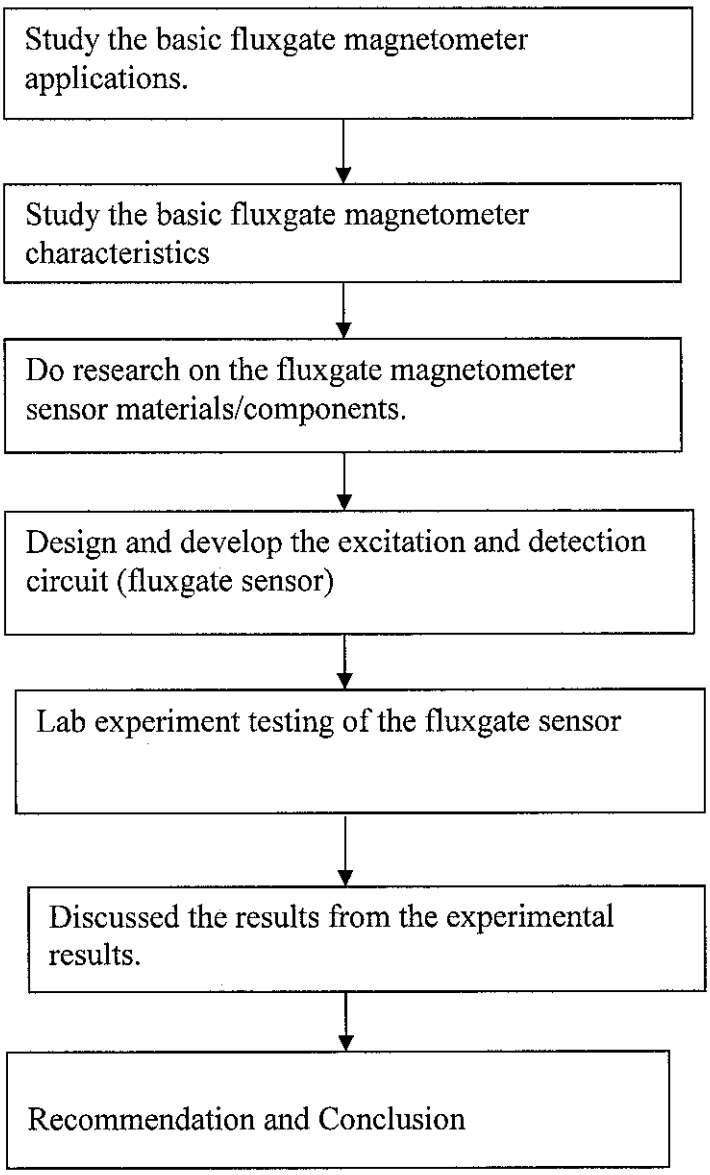


Figure 5: Flow Chart

## 3.2 Design Methodology of Hard ware

A) Build the sense/drive coils.

Wrap the magnet wire uniformly around the stovepipe wire (this is the excitation coil); they should have the same number of turns per unit length throughout the length of the stovepipe wire. The magnet wire windings need to be uniform for best results as show in figure 6.

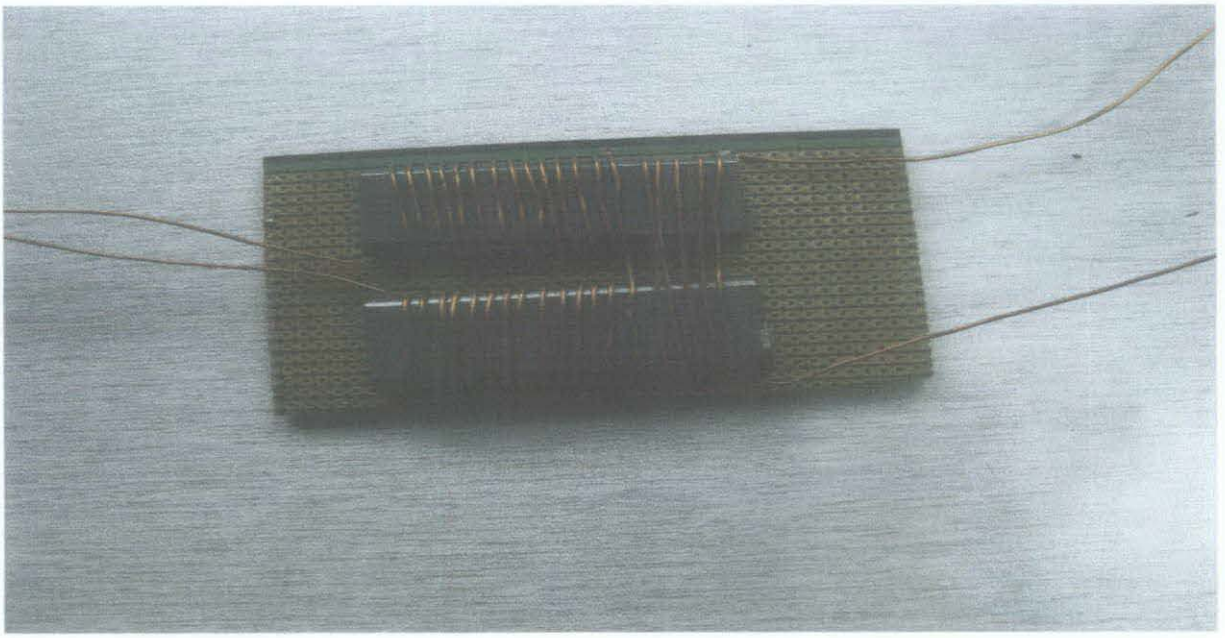

Figure 6: Rod Core sensors

Now you need to wrap some more magnet wire around the rod core shaped device, this will be the sense coil. Again try to make the windings uniform.

B) Assemble the fluxgate magnetometer.

Connect the function generator, waveform analyzer, amplifier, and oscilloscope as shown in the schematic in figure 7. Set the function generator to a triangle wave of 1000 Hz. Set the wave form analyzer to the band pass filter and set the band pass filter to 2000 Hz .Set the amplifier to an amplification of 30. Turn on the oscilloscope and adjust it to find the 2000 Hz signal. What the author has done is to filter out the second harmonic of the sense coil; this second harmonic is remarkably sensitive to small changes in the magnetic field. Orient the sensor along direction of the earth's magnetic field (You can use a dip needle and/or compass to find the earth's magnetic field), you will see the sine wave increase in magnitude, the amplitude of the sine wave (the second harmonic) is proportional to the magnetic field. You can bring a small bar magnet towards the sensor, you will again see the sine wave displayed on the oscilloscope increase in magnitude. You can calibrate the magnetometer by making a known magnetic field with a pair of Helmholtz coils.

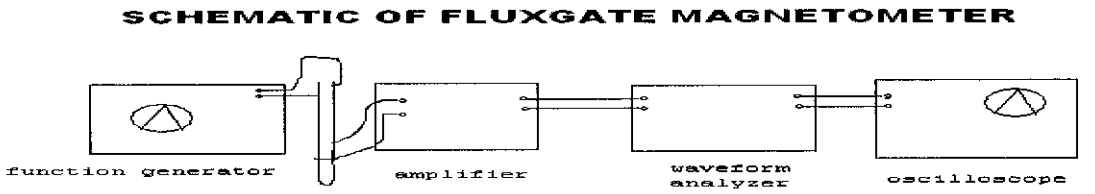


Figure 7: Schematic of fluxgate magnetometer

### 3.3.1 Tool Requirement

- PCB hard ware
- A function generator
- An oscilloscope
- D-flip flop
- Phase Locked Loop
- Band- Pass filter
- Amplifier
- A spool of magnet wire (iron wire that becomes magnetically saturated at low magnetic fields).

### 3.4 Helmholtz coil

The term **Helmholtz coils** refers to a device for producing a region of nearly uniform magnetic field. It is named in honor of the German physicist Hermann von Helmholtz.

A Helmholtz pair consists of two identical circular magnetic coils that are placed symmetrically one on each side of the experimental area along a common axis, and separated by a distance $h$ equal to the radius $R$ of the coil. Each coil carries an equal electrical current flowing in the same direction.

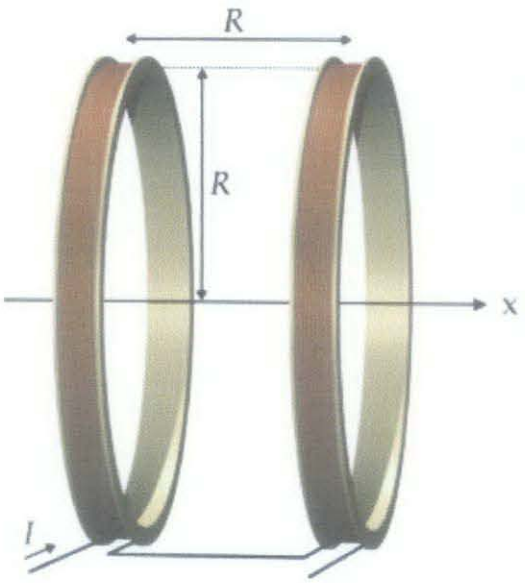


Figure 8: Helmholtz coil schematic drawing

Figure 9: Helmholtz coil

Setting $h = R$, which is what defines a Helmholtz pair, minimizes the no uniformity of the field at the center of the coils, in the sense of setting $d^2B / dx^2 = 0$, but leaves about 6% variation in field strength between the center and the planes of the coils. A slightly larger value of $h$ reduces the difference in field between the center and the planes of the coils, at the expense of worsening the field's uniformity in the region near the center, as measured by $d^2B / dx^2$

The calculation of the exact magnetic field at any point in space has mathematical complexities and involves the study of Bessel functions. Things are simpler along the axis of the coil-pair, and it is convenient to think about the Taylor series expansion of the field strength as a function of $x$, the distance from the central point of the coil-pair along the axis. By symmetry the odd order terms in the expansion are zero. By separating the coils so that $x = 0$ is an inflection point for each coil separately we can guarantee that the order $x^2$ term is also zero, and hence the leading non-uniform term is of order $x^4$. One can

easily show that the inflection point for a simple coil is $R$ / 2 from the coil center along the axis; hence the location of each coil at $x = \pm R/2$

A simple calculation gives the correct value of the field at the center point. If the radius is $R$, the number of turns in each coil is $n$ and the current flowing through the coils is $I$, then the magnetic flux density, B at the midpoint between the coils will be given by

$$B = \left(\frac{4}{5}\right)^{3/2} \frac{\mu_0 n I}{R} \quad \text{.....(2)}$$

$\mu_0$ is the permeability constant ($1.26 \times 10^{-6}$ T · m/A), and $R$ is in meters.

**Derivation**

Start with the formula for the on-axis field due to a single wire loop_(which is itself derived from the Biot-Savart law):

$$B = \frac{\mu_0 I R^2}{2(R^2 + x^2)^{3/2}} \quad \text{.....(3)}$$

Where:

$\mu_0$ is the permeability constant which is $4\pi \times 10^{-7}$ T · m/A = $1.26 \times 10^{-6}$ T · m/A

$I$ is the coil current, in amperes

$R$ is the coil radius, in meters

$x$ is the coil distance, on axis, to point, in meters

However the coil consists of a number of wire loops, the total current in the coil is given by

$nI$ is the total current

Where:

$n$ is the number of wire loops in one coil

Adding this to the formula:

$$B = \frac{\mu_0 n I R^2}{2(R^2 + x^2)^{3/2}} \quad \text{.....(4)}$$

In a Helmholtz coil, a point halfway between the two loops has an x value equal to R/2, so let's perform that substitution:

$$B = \frac{\mu_0 n I R^2}{2(R^2 + (R/2)^2)^{3/2}} \quad \text{.....(5)}$$

There are also two coils instead of one, so let's multiply the formula by 2, and then simplify the formula:

$$B = \frac{2\mu_0 n I R^2}{2(R^2 + (R/2)^2)^{3/2}} \quad \text{.....(6)}$$

$$B = \left(\frac{4}{5}\right)^{3/2} \frac{\mu_0 n I}{R} \quad \text{.....(7)}$$

### 3.5 Band-pass filter

A band-pass filter is a device that passes frequencies within a certain range and rejects attenuates frequencies outside that range. An ideal band-pass filter would have a completely flat pass-band and would completely attenuate all frequencies outside the pass-band. Moreover, the transition out of the pass-band would be instantaneous in frequency. In practical, no band-pass filter is ideal. The filter doesn't attenuate all the frequencies outside the desired frequency range completely; in particularly, there is a region just outside the intended pass-band where frequencies are attenuated, but not rejected.

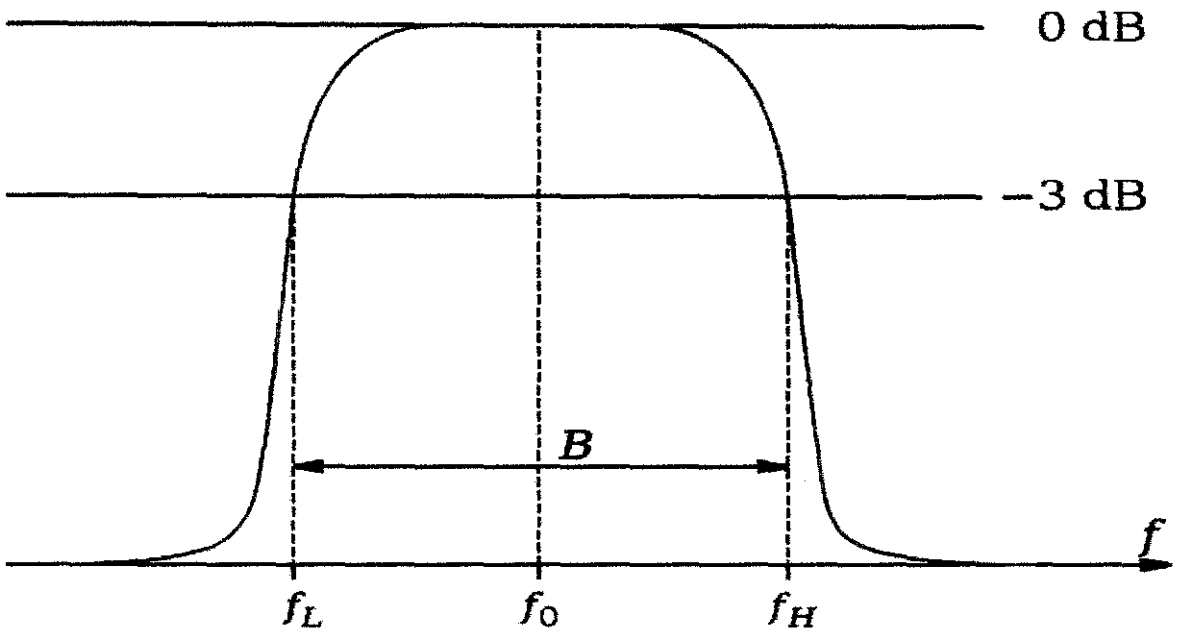


Figure 10: Magnitude transfer function versus frequency for a band-pass filter

The filter roll-off is expressed in dB of attenuation per octave or decade of frequency. Generally, the design of a filter seeks to make the roll-off as narrow as possible, thus allowing the filter to perform as close as possible to its intended design. The bandwidth of the filter is simply the difference between the upper and lower cut-off frequencies.

The author has chosen multiple feedback band-pass filters to extract the second harmonic voltage from the ferrite rod core. There are a couple of advantages to this active band-pass filter. First, it doesn't need an inductor to create the band-pass shape. Second, it only needs one operational amplifier. One disadvantage is the nature of adjusting the center frequency fo. Adjustments are not orthogonal, fo can be tuned with a resistor; but, the quality factor, Q also changes; still, the circuit is easy to implement.

Two feed-back paths are through R3 and C1. R1 and C1 provide the low pass response while R3 and C2 provide the high pass response (refer to figure 11). The maximum gain, A0 occurs at centre frequency. Quality factor, Q value of the less than 10 is the typical for this type of filter. First step to design the multiple feedback band-pass filters is to choose a convenient value for capacitor. Then the three resistors values are calculated based on the desired values for fo, BW and Ao. The maximum again, Ao must less than $2Q^2$ for R2 to be positive which imposes a limitation of the gain.

the voltage spikes passing through, and a broader band amplifier with a reasonably high slew rate can help avoid this.

Demodulation is usually accomplished with a phase sensitive detector, typically a CMOS analogue switch, following the preamp. It is important to choose a switch with low charge injection to avoid further offset problems. The switch drives an op-amp integrator, which needs to be a low offset, low temperature coefficient device. The integrator time constant is chosen as a compromise between response time and noise performance.

The feedback voltage to current converter can be as simple as a resistor, or an active device such as a transconductance amplifier can be employed. When a resistor is used, its temperature coefficient will be added directly to the magnetic field measurement, so care needs to be taken here. In addition should the voltage from the integrator be taken as the field output, the proportion of voltage across the feedback coil will be subject to the large temperature coefficient of copper. This can be taken out in software or by the use of additional analogue circuitry. Where a microprocessor is available the former solution is preferable, providing a more accurate result and less interference to the low level sense signal from the fluxgate. [11]

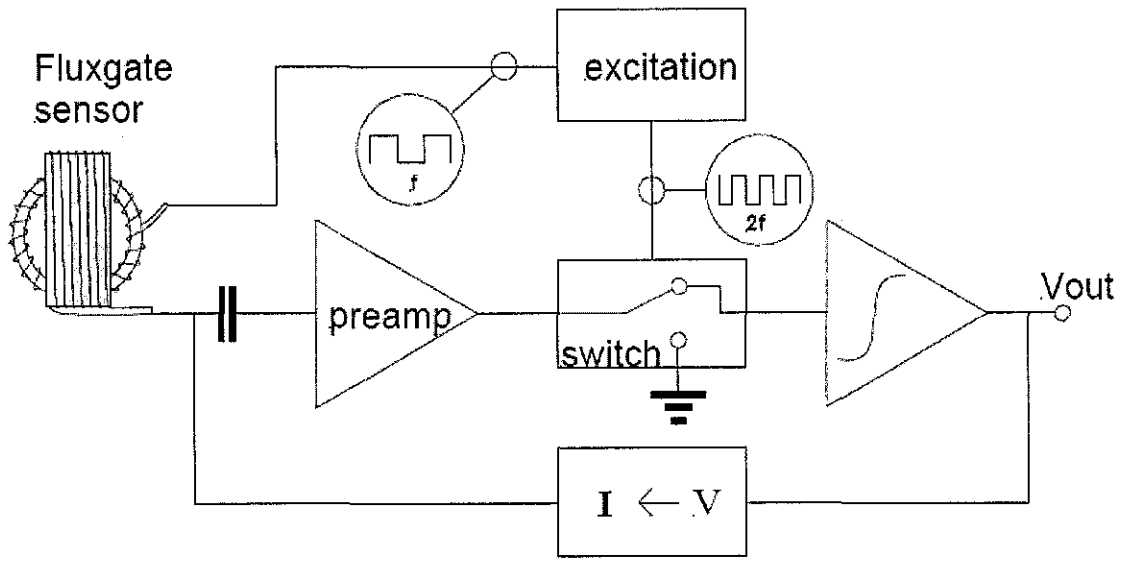


Figure 12: Classic 2nd harmonic demodulator schemes

The next step was adding the band-pass filter to the circuit in order to extract the second harmonic voltage. Below is design procedure for multiple-feedback band-pass filter

Calculation Values:

Assume R1=1KΩ

$A0=10=\frac{R3}{2R1} \rightarrow R3=(10)(2)(1K\Omega)= 20K\Omega$

Choose $fo = 10\ kHz$ , assume C1=C2=C=10nf

$$fo = \frac{1}{2\prod C}\sqrt{\frac{R1+R2}{R1R3R2}}$$

$$10\ kHz = \frac{1}{2\prod(10^{-n})}\sqrt{\frac{1k\Omega+R2}{(1k\Omega)(20\ k\Omega)(R2)}}$$

$$R2 = 145\ \Omega$$

Finally, the author has added the phase locked loop and D-flip flop to the circuit. The D-flip flop function is to divide the frequency of function generator by two. There are two frequencies which are f and 2f frequency. The f frequency is drive frequency while the 2f frequency is sense frequency. The phase locked loop function is to make sure that both frequencies and phase of the sense frequency matched to the drive frequency. The block diagram below showed the final circuit of fluxgate Sensor design. [12]

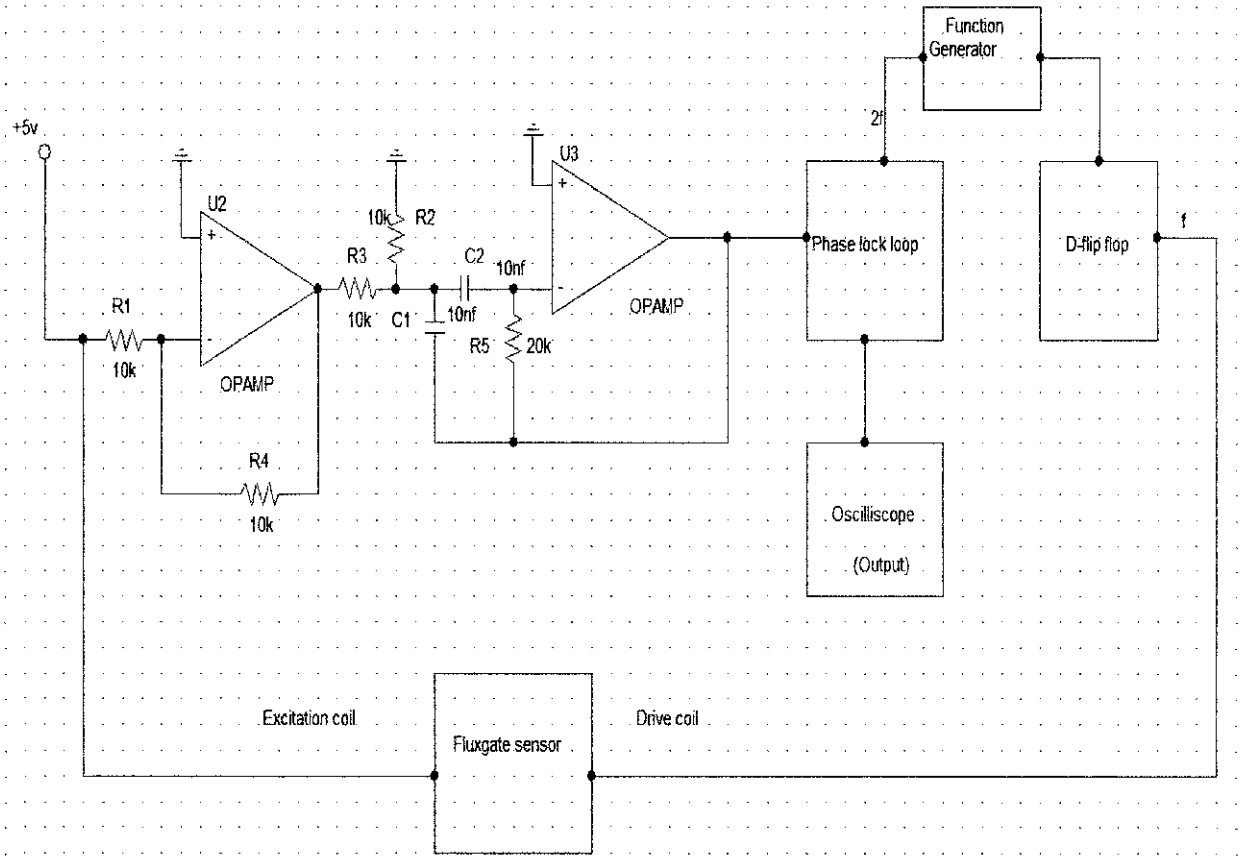


Figure 13: Schematic Diagram of fluxgate sensor

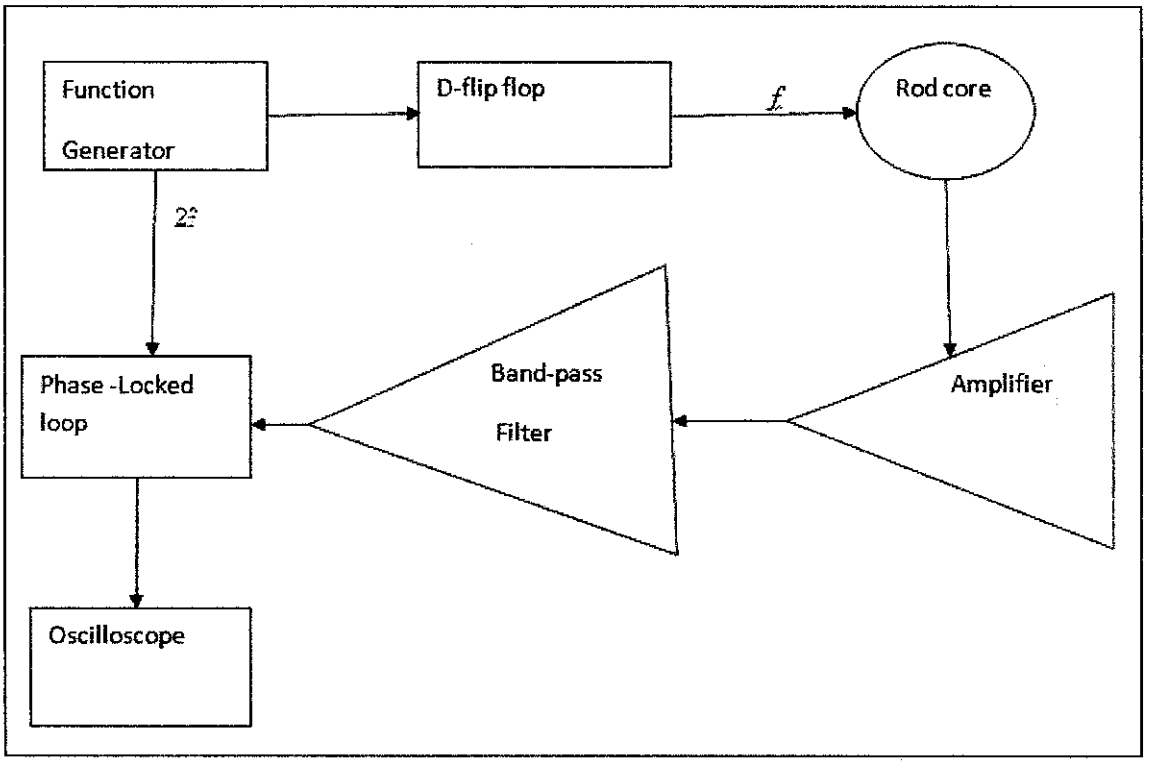


Figure 14: Block diagram of fluxgate Sensor

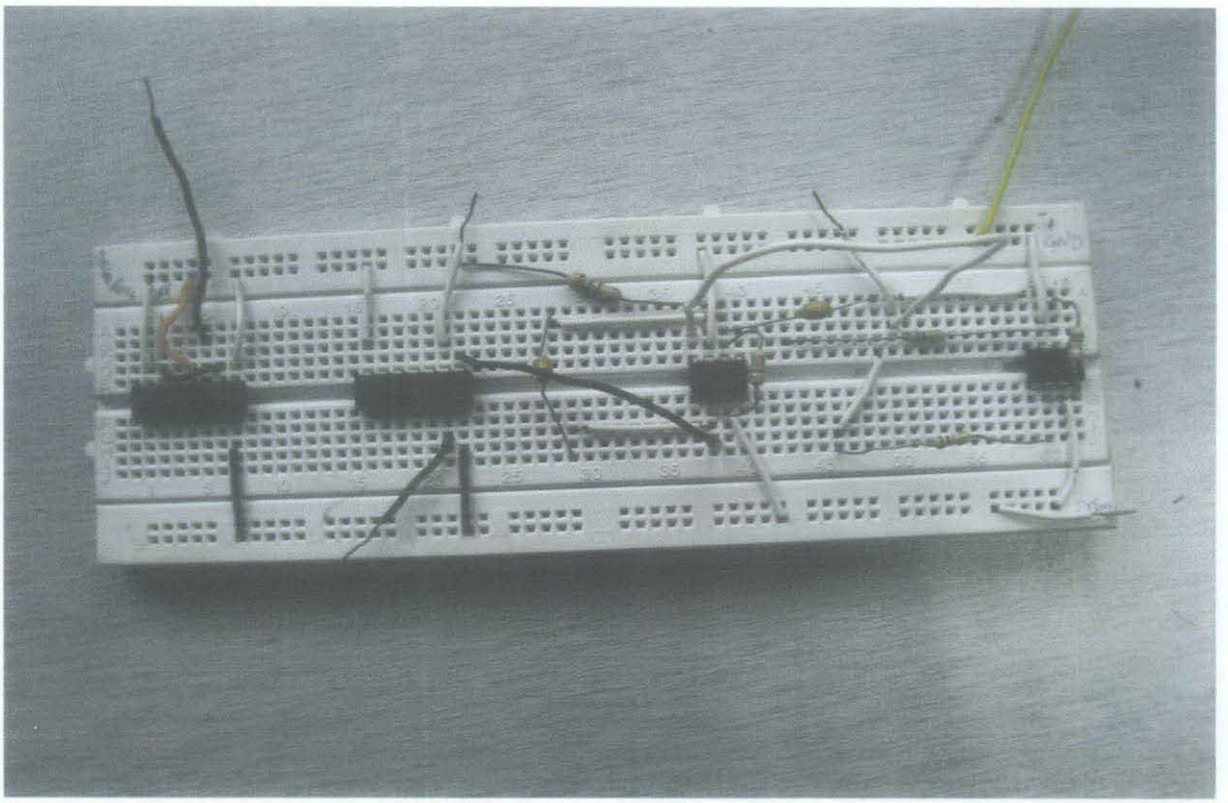

Figure 15: Fluxgate sensor circuit

### 3.7 Calibration system

Since the output of the fluxgate sensor is low frequency voltage, calibration of the fluxgate sensor is needed to determine the linearity between the output voltage and the external magnetic field. A simple calibration block using Helmholtz coil has been setup(refer to figure 15) .Helmholtz coil was used to generate known uniform magnetic fields up to 30% covered area from the centre axis if powered by a constant current source. The fluxgate sensor was placed in the centre of Helmholtz coil, see the figure 15.

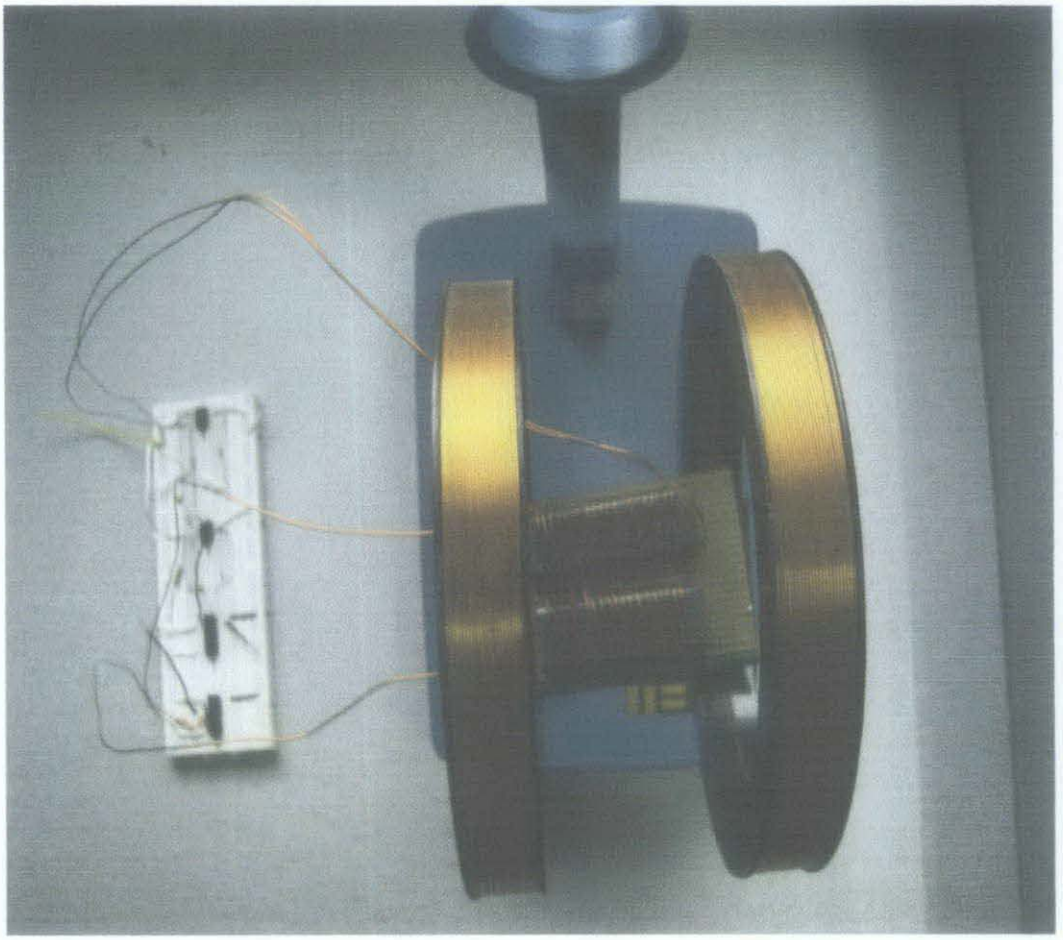

Figure 16: Calibration system

Using the formula $B=(\frac{4}{5})^{3}/_{2}\frac{\mu nI}{R}$, the external magnetic field was calculated with respect to the constant current supply that was applied to the Helmholtz coil. The calibration was done within the range of -39.09 $\mu T$ to +39.09 $\mu T$ by adjusting the constant current supply. Output of the fluxgate sensor, in volts was plotted against the magnetic field applied to the Sensor

# CHAPTER 4

## RESULTS AND DISCUSION

The result of the circuit when the author has connected the ferrite rode core directly to the oscilloscope before connected to Conditional Circuit as shown in the figure 16. The figure shows that an alternating current that is applies cancel out since the primary turns are connected in opposite direction which leads to zero harmonic voltage.

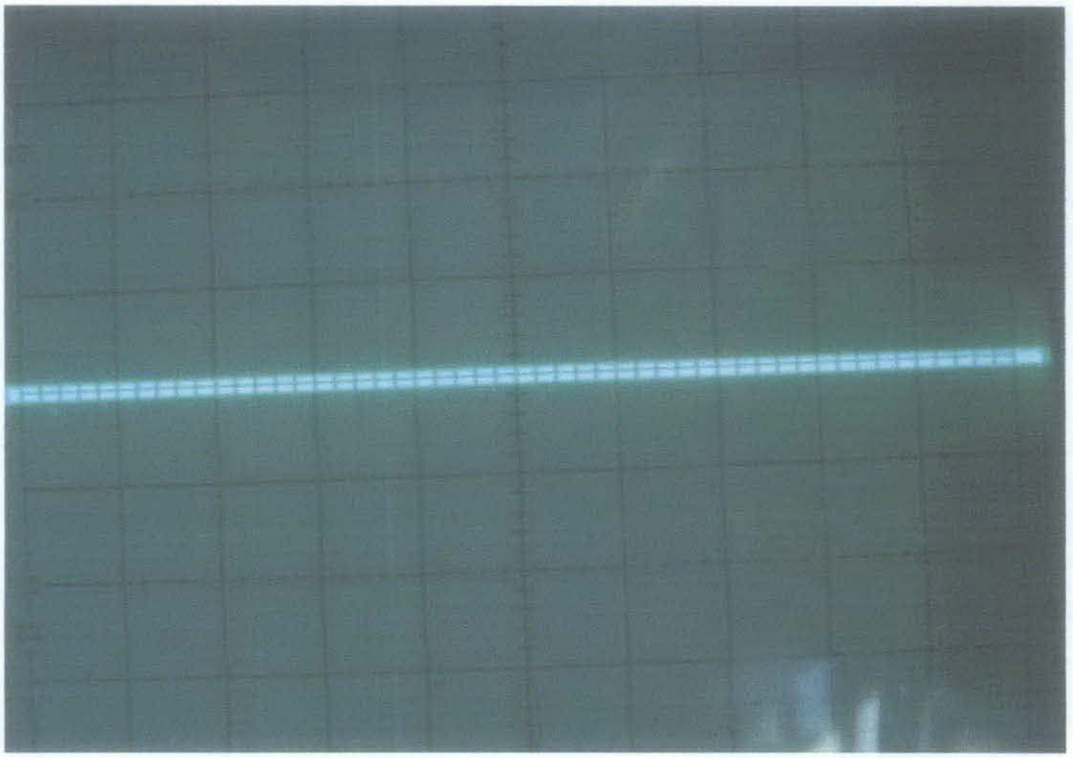

Figure 17: Alternating Current

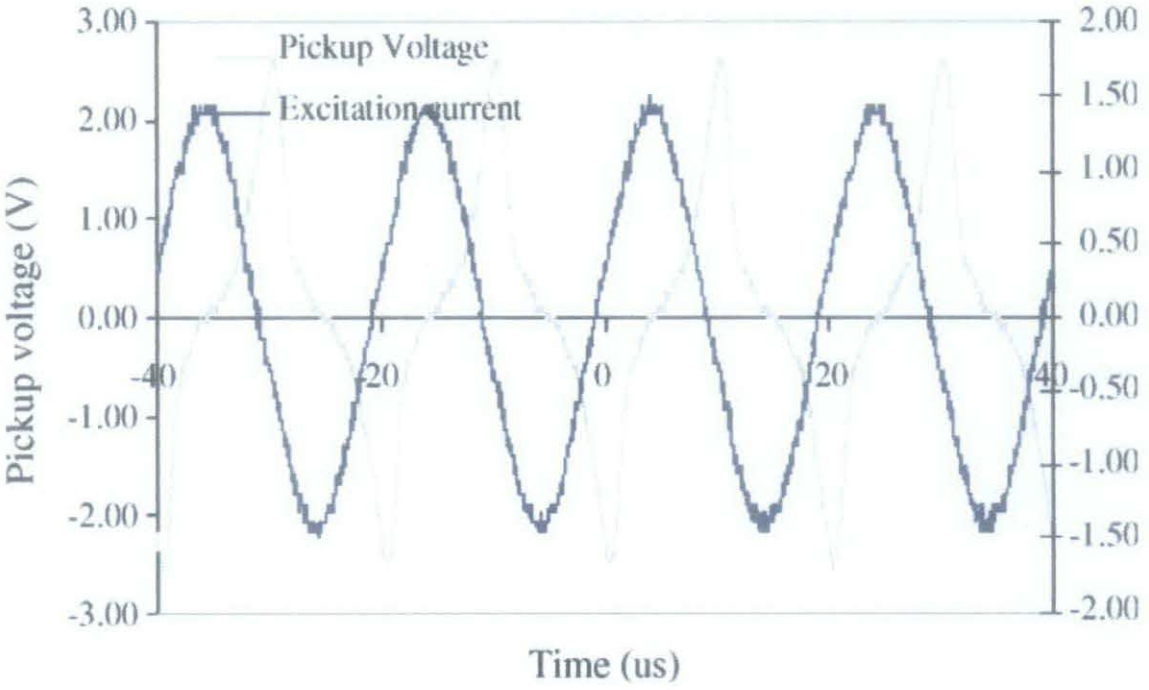


Figure 18: Drive current and pickup voltage for the sensor at 50 kHz excitation frequency.

The fluxgate sensor is tested using a sinusoidal drive current, supplied by a power supply. The pickup windings are connected in anti-series and are connected to a lock in amplifier, set to detect the second harmonic component of the voltage.

The current carrying conductor is connected to a dc current source. A peak driving current of 0.38A (as shown in figure 18) is chosen as the excitation for the sensor to ensure full saturation of the core.

The pickup voltage (Second Harmonic Voltage) for sensor at 0.38A and 50 kHz excitation frequency is shown in figure 19.

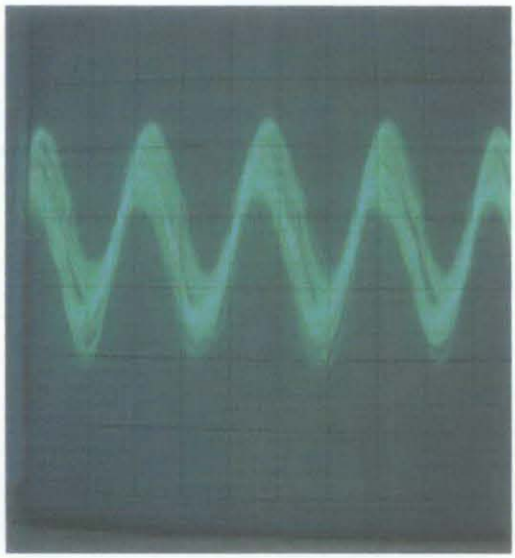

Figure 19: Drive current

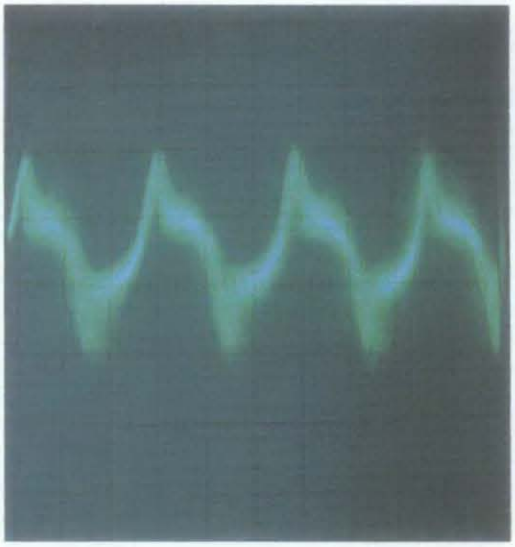

Figure 20: Pickup voltage for sensor at 50 kHz excitation frequency

The result of the fluxgate sensor in the presence of external magnetic field is shown in figure 20. We can see the magnitude of the voltage is differing from the previous one. The magnitude of the sinusoidal voltage is approximately 150 mV/A peak-to-peak.

The difference was measured and used in calibration system.

The sensitivity of the sensor is measured by varying the dc current and measuring the absolute value response of the second harmonic of the pickup voltage. This is done for two different excitation frequencies, 50 kHz and 30 kHz.

The results for a dc current range of 0.10 A are shown in Figure 20 .In each case the offset voltage of the sensor at 0A dc current is nulled using the nulling function of the lock-in amplifier and the phase was set so as to achieve a maximum output value at 0.5A dc current. The nulled offsets were 5mV and 5.1mV for 50 kHz and 30 kHz, respectively. As can be seen the sensor show linear characteristic over the 0.10 A range.

The sensitivity is approximately 150 mV/A at 50 kHz and 100 mV/A at 30 kHz. As expected the sensitivity increases with increasing excitation frequency.

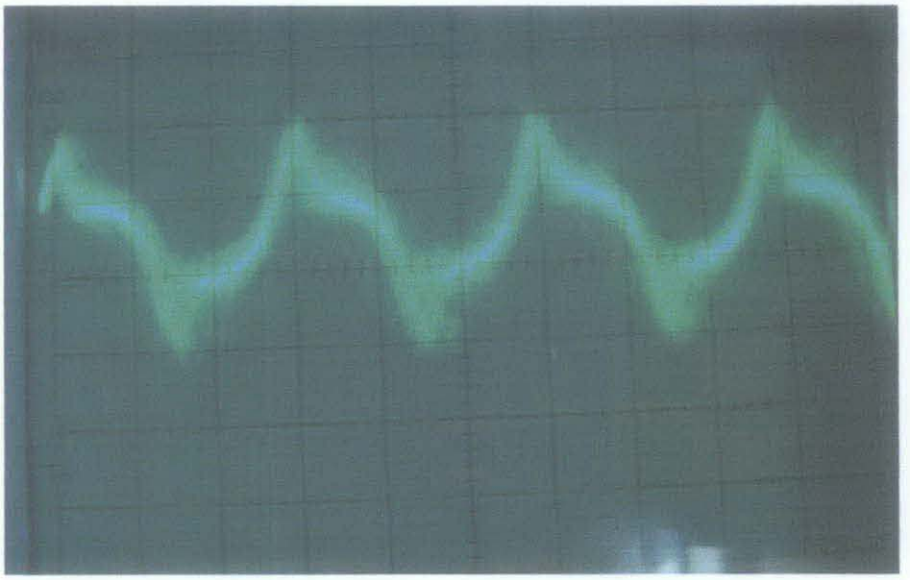

Figure 21: Second harmonic voltage with external field from Helmholtz coil

The result for the calibration system is showing table 2 and figure 20. The fluxgate was calibrated within the range of -39.09 $\mu T$ to +39.09 $\mu T$ . The output is linear

From the formula $B = \left(\frac{4}{5}\right)^{3}/_{2}\frac{\mu nI}{R}$, we can calculate the range of magnetic field, where μ0 is the permeability constant ($1.26 \times 10^{-6}$ T · m/A), n is 13 turns,

I is from -0.10 to +0.10 A, R is 0.03 in meter.

Table 2: Voltage difference for various applied magnetic field with respective current

| Current (A) | Magnetic field ( $\mu T$ ) | Voltage difference (mV) |
|---|---|---|
| -0.10 | -39.07 | -4.4 |
| -0.08 | -31.25 | -3.8 |
| -0.06 | -23.44 | -3.1 |
| -0.04 | -15.63 | -2.4 |
| -0.02 | -7.81 | -1.2 |
| 0 | 0 | 0 |
| 0.02 | 7.81 | 1.3 |
| 0.04 | 15.63 | 2.2 |
| 0.06 | 23.44 | 3.3 |
| 0.08 | 31.25 | 3.9 |
| 0.10 | 39.07 | 4.3 |

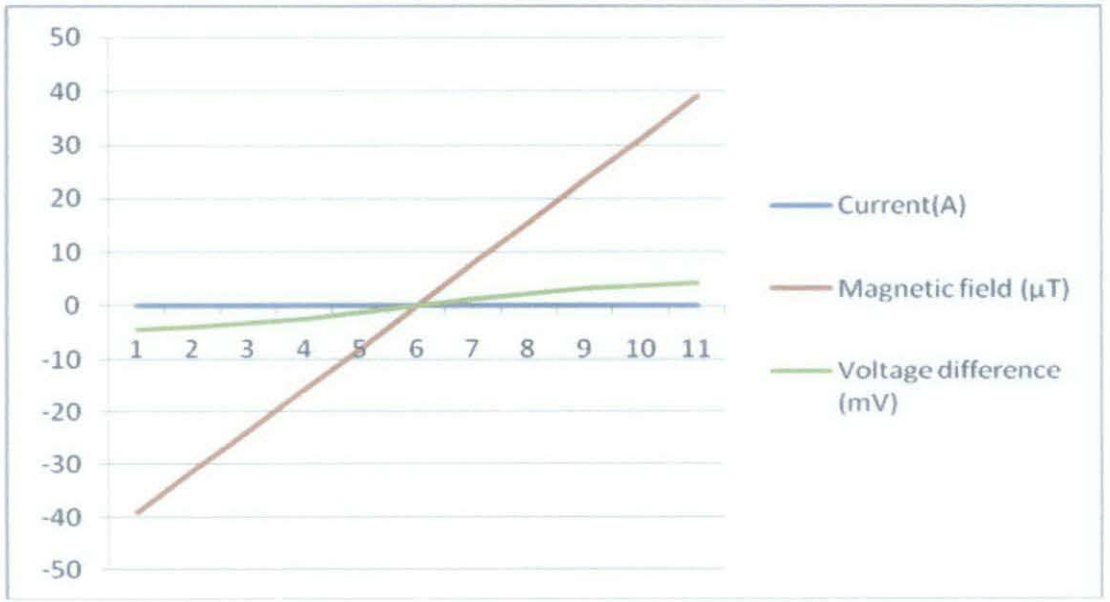


Figure 22: Voltage difference for various applied magnetic field with respective current.

# CHAPTER 5

# CONCLUSION AND RECOMMENDATION

## 5.1 Conclusion

Fluxgate magnetometers were first built in World War two for submarine and mine detection, NASA has used fluxgate magnetometers on probes to accurately measure magnetic fields of our moon and several planets in our solar system.

The design and testing of a fluxgate sensor, which is totally embedded in printed circuit board, has been presented. The sensor is suitable for sensing currents in the printed circuit board traces.

The sensitivity has been measured at 150 mV/A for 50 kHz excitation. The power dissipation has been measured at approximately 1.44 W for a sinusoidal excitation. The power dissipation reduced by using pulse excitation, or perhaps by using a saturable inductor in the excitation circuit.

It is also possible to improve the sensitivity and reduce the power consumption by use of an improved magnetic material. In particular a material with lower saturation flux density and higher permeability should be possible.

Future work will focus on further characterization of the sensor in terms of bandwidth, noise level, and minimum current detection level.

As conclusions from this research, the author still believe that fluxgate sensor is best sensor due to sensitivity to detect the magnetic fields

## 5.2 Recommendation

Further studies on the fluxgate magnetometer (Fluxgate sensor) circuit and component should be done in order to increase sensitivity of fluxgate sensor.

Since the author fluxgate has successful reduce power consumption of fluxgate sensor but not that much effort has been achieve by author in term of sensitivity of fluxgate sensor due to the component thickness that may interrupt sensitivity or other factors that may arise to reduce sensitivity, more effort need to be done in the term of sensitivity

The Author recommended more research need to been done in the Magnetic Materials properties of fluxgate sensor since they are playing a great role in the term of power reduction and sensitivity.

## REFERENCES

[1] Forster, "A method for the measurement of DC fields and DC field differences and its application to non-destructive testing," Nondestruct. Test., vol.13, pp. 31—41, Sept.-Oct. 1955

[2] Vacquier, et al, "A magnetic airborne detector employing magnetically controlled gyroscopic stabilization," Rev. &i.Instrurn., vol. 18pp. 483-487,1947

[3] Geyger, W. A., "The Ring Core Magnetometer - A New Type of Second-Harmonic Flux-Gate", AIEE Trans.Communications and Electronics, 81, pp65-73, 1962

[4] Ripka: "New Directions in Fluxgate Sensors", JMMM (2000) 215-216 (2000), 735-739

[5] Fluxgate Magnetometry, R. Noble, Electronics World + Wireless World (Sept. 1991) vol. 97, p.726-32.

[6] A Review of Magnetic Sensors, J.E. Lenz, Proc. IEEE 78(6) 1990 p.973.

[7] Recent Advances in Fluxgate Magnetometry, D.I. Gordon, R.E. Brown, IEEE Trans. Magnetics v. MAG-8,1, 1972 p. 76-82

[8] Earths Field Magnetometry, W.F. Stuart, Reports on Progress in Physics, 1972, vol. 35, p.803-881.

[9] Magnetic Measurements Handbook, J.M. Janicke, Magnetic Research Press 2nd edition 1997.

[10] Electricity and Magnetism ,E. Purcell, McGraw Hill 2nd edition 1985, p 397-450.

[11] Novel Medical Imaging Shows Promise, Charles Day, Physics Today, 58(9) p. 21-22.

[12] Atom Based Detector Puts New Twist on Nuclear Magnetic Resonance, Adrian Cho, Science 25 March 2005, 307: 1855.6

## APPENDIX A: Datasheet

SGS-THOMSON MICROELECTRONICS

# UA741

## GENERAL PURPOSE SINGLE OPERATIONAL AMPLIFIER

- LARGE INPUT VOLTAGE RANGE
- NO LATCH-UP
- HIGH GAIN
- SHORT-CIRCUIT PROTECTION
- NO FREQUENCY COMPENSATION REQUIRED
- SAME PIN CONFIGURATION AS THE UA709

N
DIP8
(Plastic Package)

D
SO8
(Plastic Micropackage)

### DESCRIPTION

The UA741 is a high performance monolithic operational amplifier constructed on a single silicon chip. It is intented for a wide range of analog applications.

- Summing amplifier
- Voltage follower
- Integrator
- Active filter
- Function generator

The high gain and wide range of operating voltages provide superior performances in integrator, summing amplifier and general feedback applications. The internal compensation network (6dB/octave) insures stability in closed loop circuits.

### ORDER CODES

| Part Number | Temperature Range | Package | |
|---|---|---|---|
| | | N | D |
| UA741C | 0°C, +70°C | • | • |
| UA741I | -40°C, +105°C | • | • |
| UA741M | -55°C, +125°C | • | • |
| Example : UA741CN | | | |

### PIN CONNECTIONS (top view)

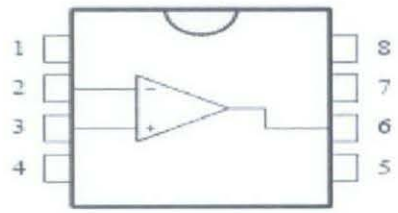


1 - Offset null 1
2 - Inverting Input
3 - Non-inverting Input
4 - $V_{CC}^-$
5 - Offset null 2
6 - Output
7 - $V_{CC}^+$
8 - N.C.

## DESCRIPTION

The HEF4066B has four independent bilateral analogue switches (transmission gates). Each switch has two input/output terminals (Y/Z) and an active HIGH enable input (E). When E is connected to $V_{DD}$ a low impedance bidirectional path between Y and Z is established (ON condition). When E is connected to $V_{SS}$ the switch is disabled and a high impedance between Y and Z is established (OFF condition).

The HEF4066B is pin compatible with the HEF4016B but exhibits a much lower ON resistance. In addition the ON resistance is relatively constant over the full input signal range.

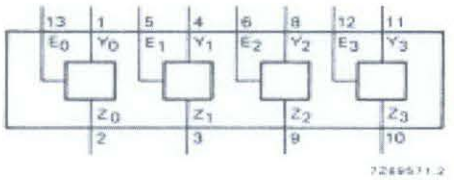


Fig.1 Functional diagram.


Fig.2 Pinning diagram.

HEF4066BP(N): 14-lead DIL; plastic (SOT27-1)
HEF4066BD(F): 14-lead DIL; ceramic (cerdip) (SOT73))
HEF4066BT(D): 14-lead SO; plastic (SOT108-1)
( ): Package Designator North America

## PINNING

$E_0$ to $E_3$ enable inputs
$Y_0$ to $Y_3$ input/output terminals
$Z_0$ to $Z_3$ input/output terminals

## APPLICATION INFORMATION

An example of application for the HEF4066B is:

- Analogue and digital switching

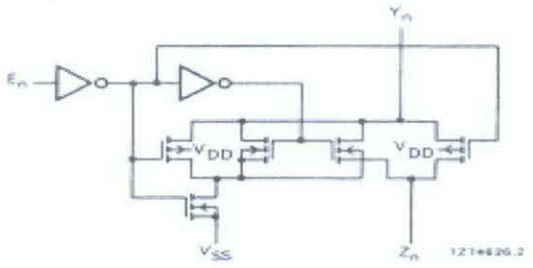


Fig.3 Schematic diagram (one switch).

# SN54HC74, SN74HC74
# DUAL D-TYPE POSITIVE-EDGE-TRIGGERED FLIP-FLOPS WITH CLEAR AND PRESET

SCLS004D – DECEMBER 1982 – REVISED JULY 2003

- Wide Operating Voltage Range of 2 V to 6 V
- Outputs Can Drive Up To 10 LSTTL Loads
- Low Power Consumption, 40-μA Max $I_{CC}$
- Typical $t_{pd}$ = 15 ns
- ±4-mA Output Drive at 5 V
- Low Input Current of 1 μA Max

SN54HC74 . . . J OR W PACKAGE
SN74HC74 . . . D, DB, N, NS, OR PW PACKAGE
(TOP VIEW)

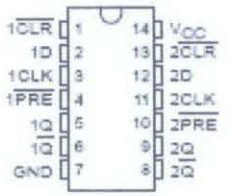


SN54HC74 . . . FK PACKAGE
(TOP VIEW)

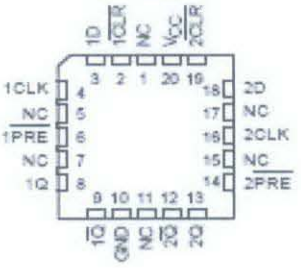


NC – No internal connection

## description/ordering information

The 'HC74 devices contain two independent D-type positive-edge-triggered flip-flops. A low level at the preset ($\overline{PRE}$) or clear ($\overline{CLR}$) inputs sets or resets the outputs, regardless of the levels of the other inputs. When $\overline{PRE}$ and $\overline{CLR}$ are inactive (high), data at the data (D) input meeting the setup time requirements are transferred to the outputs on the positive-going edge of the clock (CLK) pulse. Clock triggering occurs at a voltage level and is not directly related to the rise time of CLK. Following the hold-time interval, data at the D input can be changed without affecting the levels at the outputs.

ORDERING INFORMATION

| $T_A$ | PACKAGE† | | ORDERABLE PART NUMBER | TOP-SIDE MARKING |
|---|---|---|---|---|
| –40°C to 85°C | PDIP – N | Tube of 25 | SN74HC74N | SN74HC74N |
| | SOIC – D | Tube of 50 | SN74HC74D | HC74 |
| | | Reel of 2500 | SN74HC74DR | |
| | | Reel of 250 | SN74HC74DT | |
| | SOP – NS | Reel of 2000 | SN74HC74NSR | HC74 |
| | SSOP – DB | Reel of 2000 | SN74HC74DBR | HC74 |
| | TSSOP – PW | Tube of 90 | SN74HC74PW | HC74 |
| | | Reel of 2000 | SN74HC74PWR | |
| | | Reel of 250 | SN74HC74PWT | |
| –55°C to 125°C | CDIP – J | Tube of 25 | SNJ54HC74J | SNJ54HC74J |
| | CFP – W | Tube of 150 | SNJ54HC74W | SNJ54HC74W |
| | LCCC – FK | Tube of 55 | SNJ54HC74FK | SNJ54HC74FK |

† Package drawings, standard packing quantities, thermal data, symbolization, and PCB design guidelines are available at www.ti.com/sc/package